

# Structure of a tethered polymer under flow using molecular dynamics and hybrid molecular-continuum simulations

Rafael Delgado-Buscalioni and Peter V. Coveney

*Centre for Computational Science, Dept of Chemistry, University College London,  
London UK, WC1H 0AJ*

---

## Abstract

We analyse the structure of a single polymer tethered to a solid surface undergoing a Couette flow. We study the problem using molecular dynamics (MD) and hybrid MD-continuum simulations, wherein the polymer and the surrounding solvent is treated via standard MD, and the solvent flow farther away from the polymer is solved by continuum fluid dynamics (CFD). The polymer represents a freely jointed chain (FJC) and is modelled by Lennard-Jones (LJ) beads interacting through the FENE potential. The solvent (modelled as a LJ fluid) and a weakly attractive wall are treated at the molecular level. At large shear rates the polymer becomes more elongated than predicted by existing theoretical scaling laws. Also, along the normal-to-wall direction the structure observed for the FJC is, surprisingly, very similar to that predicted for a semiflexible chain. Comparison with previous Brownian dynamics simulations (which exclude both solvent and wall potential) indicate that these effects are due to the polymer-solvent and polymer-wall interactions. The hybrid simulations are in perfect agreement with the MD simulations, showing no trace of finite size effects. Importantly, the extra cost required to couple the MD and CFD domains is negligible.

*Key words:* Tethered polymers, shear flow, surface phenomena, hybrid modelling, molecular dynamics, continuum fluid dynamics.

---

## 1 Introduction

If a polymer molecule is subject to a sufficiently strong hydrodynamic flow it becomes deformed and stretched. The deformation of polymers attached to surfaces is of great interest for many applications such as colloidal stabilisation, lubrication, chromatography, manufacture of composites and so on [1]. It is also relevant for biological systems, where molecules can protrude from

lipid bilayer membranes [2]. In most cases these applications involve shearing of the tethered polymer. Flow-induced changes in the polymer conformations in a dilute solution can be dramatic, and are assumed to be responsible for the existence of important macroscopically observable phenomena [3]. Indeed, the structure and dynamics of a single tethered polymer subject to flow, has attracted the attention of several groups in recent years and their work provides new insights into polymer physics (see Refs. [1,2,4,3] and references therein).

It is now possible to observe the motion of individual DNA chains by fluorescence videomicroscopy [1,4]. These sort of experiments enable scientists to investigate the dynamic properties of individual DNA chains in a shear flow, either tethered to a wall [1] or free [4]. Molecular dynamics (MD) simulations of polymeric processes are very computationally expensive because of the long time scales associated with polymer motion. Hence, most used molecular simulations of single chains under flow have been using Brownian dynamics (BD) [2,3], without considering explicit solvent and many without considering any hydrodynamic representation. The single tethered polymer was also studied using an alternative to the BD method which models the effect of the solvent-polymer interaction using the so-called collision dynamics method [3]. This method uses virtual solvent particles which produce instantaneous changes in the velocities of the beads, taken from a Maxwell distribution at the local flow velocity. However, this reductionist approach is still far from being truly atomistic: it does not take into account the solvent structure and the long-range solvent-polymer interactions and does not include hydrodynamic effects. A third alternative is to use hybrid particle-continuum simulations which treat the region around the polymer chain in fully atomistic detail, while dynamically coupling this MD region to a continuum-fluid-dynamics (CFD) solution of the solvent flow in the bulk [5,6]. Recently, our group used the hybrid approach to study a tethered polymer under shear flow and compared it with results obtained via standard MD [7]. We found excellent agreement, showing that the hybrid model can avoid finite size effects in quite small MD domains. A relevant feature of the hybrid scheme is that the computational cost required to couple the CFD and MD models is quite small (less than 5% of the grand simulation total). A key ingredient of the hybrid model is its ability to exchange mass (and energy) with the contiguous continuum region [8]. In the tethered polymer problem this mass exchange capability allows us to eliminate the solvent density waves produced by the polymer motion from the MD domain [7]. More generally it can consistently include hydrodynamic interactions with the bulk flow, further away from the MD simulation subdomain.

## 2 Method

In this article we focus on the analysis of the polymer structure obtained from our hybrid and MD simulations. Hence we shall describe only the details of the polymer, solvent and wall models, and refer to Barsky *et al.* [7] for a full technical description of the present simulations and to Delgado-Buscalioni and Coveney [5,9] for the theoretical foundation of the hybrid model. The system considered is depicted in Fig. 1. A fluid fills the space between two walls and, due to the motion of the upper wall, is subject to a constant shear. A single non-extensible polymer of contour length  $L$  is tethered to the bottom wall and interacts with the solvent flow and the bottom wall. The polymer model is based on the bead-spring model developed by Kremer and Grest [10] and contains  $N = 60$  monomer beads linked along a chain with the FENE potential  $U_{nn}(r_{ij}) = -\frac{1}{2}kR_0^2 \ln [1 - (r_{ij}/R_0)^2]$  for  $r_{ij} < R_0$ , and  $U_{nn} = \infty$  otherwise. Here  $r_{ij}$  is the distance between neighbouring beads  $i$  and  $j = i \pm 1$ ,  $R_0 = 1.5\sigma$ ,  $k = 30\epsilon/\sigma^2$ ,  $\sigma$  and  $\epsilon$  setting the length and energy scales respectively. The polymer is anchored to the wall by enforcing the same FENE potential between the tethered end of the polymer and one wall atom. The monomers in the solvent and in the polymer interact through a purely repulsive LJ potential  $U_{LJ}(r_{ij}) = 4\epsilon [(\sigma/r_{ij})^{12} - (\sigma/r_{ij})^6]$  for  $r_{ij} < 2^{1/6}\sigma$  and  $U_{LJ} = 0$  for  $r_{ij} \geq 2^{1/6}\sigma$ . The wall-fluid and wall-polymer interactions are LJ with an increased cutoff,  $r_c 1.25\sigma$ , and energy scale  $\sqrt{1.7}\epsilon$ . The momentum equation for the solvent flow within the continuum region (C) was solved by a finite volume method [7,9] while the equations of motion of the particles were integrated using a velocity Verlet algorithm with a time step  $\delta t = 0.0075\tau$ , where  $\tau \equiv \sigma\sqrt{m/\epsilon}$  and  $m$  is the mass of a monomer. A constant temperature of  $k_B T = 1.0\epsilon$  (where  $k_B$  is the Boltzmann constant) is maintained with a Langevin thermostat added to the equations of motion for the velocity components normal to the mean flow. The mean fluid density is approximately  $\rho = 0.8\sigma^{-3}$  in the bulk fluid, although density oscillations are induced within a few  $\sigma$  of the walls [7]. The present set up contrasts with previous published simulations of similar systems [2,3], which considered purely reflecting walls and no explicit solvent.

## 3 Results and analysis

For the FENE potential considered here the contour length of the polymer  $L = (N - 1)b$  (where  $b \cong 0.965$  is the bead-to-bead distance) is nearly independent of the the shear rate. The tethered polymer can be assumed to behave according to Rouse dynamics [2,11] with its longest relaxation time given by the Rouse time under no-flow conditions [12]  $\tau_0(0) = \tau_{blob}(4N^2/\pi^2) = 2294\tau$ , where  $\tau_{blob} = \eta_s b^3/k_B T \simeq 1.54\tau$  is the relaxation time of one blob (i.e., one

bead for our FENE polymer) and  $\eta_s \simeq 1.75$  is the solvent viscosity. As in experiments [2,1], we estimated  $\tau_0$  by fitting the autocorrelation of the polymer extension to an exponential function of form  $A + B \exp(-t/\tau_0)$ . We obtained  $\tau_0(0) = (2000 \pm 500)\tau$ .

In order to provide insight into the foregoing analysis we introduce the basic scaling laws derived by previous authors [2,11]. To fix terminology we define the average polymer extension along any direction  $\vec{e}$  as  $E \equiv \langle \max \vec{R}_n \cdot \vec{e} - \min \vec{R}_n \cdot \vec{e} \rangle$ , where  $\vec{e}$  is unit vector,  $\vec{R}_n$  is the position of the  $n^{\text{th}}$  bead and brackets denote the average over a long time interval ( $\gtrsim O(10)\tau_0$ ). In particular  $X$ ,  $Y$  and  $Z$  denote the average chain extensions along the longitudinal (flow) direction ( $x$ ), the normal-to-wall direction ( $y$ ) and the vorticity or neutral direction ( $z$ ), respectively. The two transversal directions are  $y$  and  $z$ .

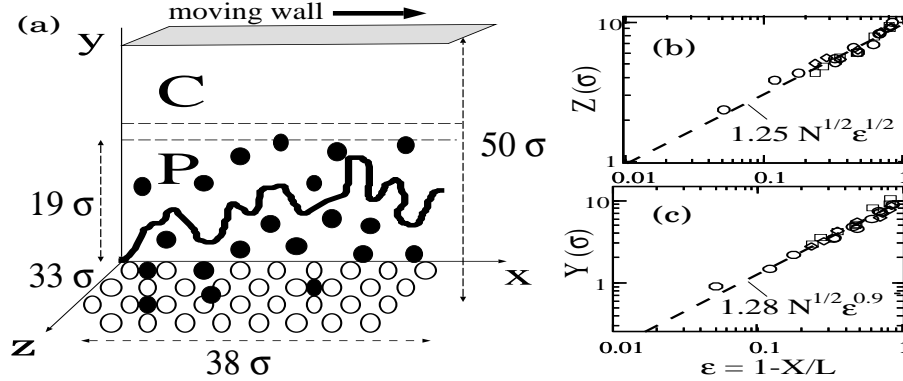


Fig. 1. (a) The set up for the tethered polymer and the domain decomposition of the hybrid scheme. The simulation cell is periodic in the  $x$  and  $y$  directions and bounded in the  $y$  direction by upper and lower walls. The shear flow is induced by moving the top wall at a constant velocity,  $u_{wall}$ . In the hybrid simulations the polymer is embedded within the molecular dynamics region (P), including the atomistic (lower) wall and the explicit solvent. The continuum fluid dynamics domain (C) comprises the upper part of the simulation cell and the exchange of mass and momentum between C and P is performed in the overlapping region (between dashed lines). (b) and (c) The averaged transversal extensions of the chain ( $N = 60$  beads) normalised with the contour length,  $L$ , versus the extensional parameter  $\epsilon = 1 - X/L$ . Here,  $X$  is the average extension along the flow direction,  $Z$  that along the vorticity direction (b) and  $Y$  that along the normal-to-wall direction (c). Data correspond to both standard MD and MD/CFD hybrid simulations, with symbols as in Fig. 2.

The relevant non-dimensional parameters are the extensional parameter,  $\epsilon \equiv 1 - X/L$  and the Weissenberg number  $Wi \equiv \dot{\gamma}\tau_0(0)$ . For a stretched polymer  $\epsilon \sim 0$ , while for a coiled configuration  $\epsilon \sim 1$ . The Weissenberg number is the ratio of the longest polymer relaxation time to the characteristic time for a significant deformation (shearing) of a fluid element,  $1/\dot{\gamma}$ . For  $Wi > 1$ , the polymer is significantly affected by the shear flow because the fluid element around it deforms at a faster rate than the polymer can possibly relax. These non-dimensional parameters enable ready comparison between various exper-

imental data and/or simulation results. An important quantity is the force required to stretch a polymer to an elongation  $X$ , denoted  $F(X)$ . This force depends on the polymer flexibility: a flexible polymer or freely jointed chain (FJC) can be modelled using the FENE potential for which the interaction between beads yields  $F_{FJC}(X) \propto -(X/L)/(1 - (X/L)^2)$  [2]. For a stretched polymer  $\epsilon \ll 1$ , the leading term of the force expansion in  $\epsilon$  gives  $F_{FJC} \sim \epsilon$ . For semiflexible polymers or worm-like chains (WLC) such as DNA, this relationship is  $F_{WLC} \sim \epsilon^{-2}$  [2]. The spring constant of the polymer also plays a crucial rôle. Using a simple geometric argument, Hatfield and Quake [11] showed that, for a stretched polymer, the effective spring constant associated with transversal extension is given by  $k_{\perp} = F(X)/X$  while for longitudinal elongation the standard relation holds  $k_{\parallel} = (\partial F(x)/\partial x)_{x=X}$ . Note that under small stretching  $F(X)$  is linear and  $k_{\perp} = k_{\parallel}$ , but the non-linear nature of  $F(X)$  will lead to anisotropy of the polymer spring and relaxation times at moderate or large extensions.

Using these results, Ladoux and Doyle [2] presented an order of magnitude analysis for the scaling of the polymer elongation *versus* the shear rate. The rationale is that the amplitude of the chain fluctuation along the transversal directions is determined by the balance between the spring energy  $\frac{1}{2}k_{\perp}Y^2$  and the thermal energy  $k_B T$ . Using  $k_{\perp} = F/X$  and the asymptotic trends for  $F = F(\epsilon)$  mentioned above, one obtains a scaling relationship for the polymer extension along the transversal direction ( $Y$  or  $Z$ ) with  $\epsilon$ . Also, the elongations force is given by the drag due to the flow,  $F \sim \xi \dot{\gamma} Y$ , which provides the relation between  $\epsilon$  and shear rate,  $\dot{\gamma}$ , or equivalently  $Wi = \dot{\gamma} \tau_0$ . In summary, Ladoux and Doyle concluded that for a FJC,  $Y \sim Z \sim \epsilon$  and  $\epsilon \sim Wi^{-1/3}$ ; while for a WLC,  $Y \sim Z \sim \epsilon^{1/2}$  and  $\epsilon \sim Wi^{-2/3}$ .

In Fig. 1b,c we plot the average fractional extension of the polymer along the transversal directions  $Y/L$  and  $Z/L$  against  $\epsilon$ . The simulations show that along the vorticity direction  $z$  the polymer spreads like  $Z \simeq N^{1/2}\epsilon$ , where  $N = 60$ . This trend agrees perfectly with the argument proposed by Hatfield and Quake [11], which assumes that the polymer spreads like a random walker. The  $\epsilon^{1/2}$  dependence also agrees with the Ladoux and Doyle prediction for a flexible chain. But, perhaps surprisingly, the elongation along the normal-to-wall direction follows a trend which is quite similar to that predicted for a worm-like, semiflexible chain,  $Y \sim \epsilon$ . The best fit to our results gives  $Y \simeq N^{1/2}\epsilon^{0.91}$ . We believe that this “worm-like” behaviour observed in the chain structure along the  $y$  direction is due to the constraints imposed by the presence of the wall. First, the steric repulsion of the wall biases the conformations of the polymer toward positive definite  $y$  coordinate values so the polymer walk in the direction perpendicular to the wall is not truly random. Second, the polymer is compressed along the wall by the drag due to the shear flow and this may also decrease its effective flexibility along the normal-to-wall direction.

The values of  $\epsilon$  obtained in our simulations are plotted against  $Wi$  in Fig. 2a. Figure 2a also shows the scaling laws proposed by Ladoux and Doyle [2], the experimental data obtained for DNA chains under shear flow by Doyle *et al.* [1] and the results of Brownian dynamics simulations (BD) of a FJC performed by Ladoux and Doyle [2]. Note that for low-to-moderate values of  $Wi$  the flexible (FENE) chain and the semiflexible one (DNA) stretch in a similar way, in good agreement with the prediction of the WLC model  $\epsilon \simeq Wi^{-1/3}$ . The flexible chain becomes more stretched than the semiflexible chain at larger shear rates ( $Wi > 20$ ). Brownian dynamics simulations of a FJC agree perfectly with the theoretical trend, giving  $\epsilon \simeq 2.5Wi^{-2/3}$ . In this regime, our results (for a FENE chain) are consistent with the predictions for the FJC up to  $Wi \lesssim 100$ , but clearly deviate from  $Wi^{-2/3}$  for  $Wi \gtrsim 100$ , the polymer becoming more stretched than is found in BD simulations. The main difference between our model and the one used in BD simulations is the inclusion of molecular interactions between the polymer and the solvent and the attractive wall interaction. Not unexpectedly, the discrepancies between the atomistic and BD simulations become noticeable once the width in the normal-to-wall direction becomes comparable to the cutoff distance for the wall-polymer interaction,  $r_c = 1.25\sigma$ . Indeed, a glance at Fig. 2b, where our results for  $Y$  are plotted against  $Wi$ , shows that this also takes place at  $Wi \sim 100$ .

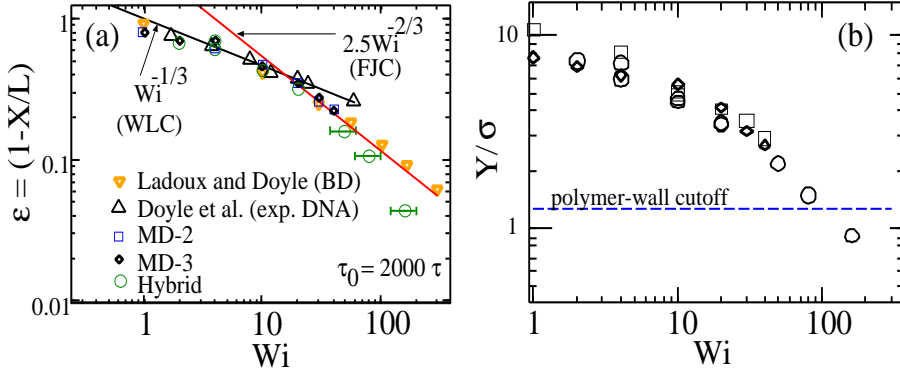


Fig. 2. (a) The extensional parameter  $\epsilon$  versus the Weissenberg number,  $Wi = \tau_0 \dot{\gamma}$ , where  $\dot{\gamma}$  is the shear rate and the longest polymer relaxation time at  $\dot{\gamma} = 0$  is  $\tau_0 = 2000 \pm 500\tau$  (the horizontal error bars shown come from the uncertainty in  $\tau_0$ ). Results obtained with the MD/CFD hybrid model are shown along with results from two independent standard MD simulations (MD-2 and MD-3). Brownian dynamics simulations by Ladoux et Doyle [2] and data from experiments on tethered DNA under shear flow by Doyle *et al.* [1] are also shown. (b) Polymer extension along the normal-to-wall direction, in units of the bead radius,  $\sigma$ , against  $Wi$ . The horizontal dashed line corresponds to the cutoff radius for the bead-wall interaction,  $r_c = 1.25\sigma$ .

The standard deviation of the polymer mean fractional extension along the flow direction  $\sigma_X$  is plotted in Fig. 3 versus the Weissenberg number. Results from the experiments by Doyle *et al.* have also been included. According to our results, the size of the fluctuations of a flexible chain attain a maximum value at  $Wi \simeq 4$ . This value is quite similar to that reported by Doyle *et al.*

for semiflexible chains (DNA),  $Wi = 5.1$ . As shown in Fig. 3, at this value of the Weissenberg number, the relative size of the fluctuations of the flexible chain are somewhat larger than those of a semiflexible polymer although the flexible polymer fluctuates less at large shear rates. The maxima of  $\sigma_X$  have been explained as a consequence of so-called “shear enhanced fluctuations” [1]. Polymer fluctuations along the positive  $y$  direction are converted by the flow into fluctuations along the flow direction  $x$  and enhanced by a factor  $\dot{\gamma}$ . At high shear rates the polymer is compressed against the wall and its extensional fluctuations decrease. This explains why the maxima of  $\sigma_X$  are found at moderate  $Wi$ , for both flexible and semiflexible chains. We found that the volume of real space that the polymer explores scales almost perfectly with the standard deviation of the extension along the flow direction. The polymer accessible volume can be estimated from the product of the polymer average extension in each direction:  $V = X \times Y \times Z$ . This volume is plotted in Fig. 3b against the Weissenberg number together with  $\sigma_X$ . A quasi perfect match  $V = 0.09\sigma_X L^2$  is found for  $Wi < 50$ , while at large  $Wi$ ,  $\sigma_X$  scales roughly like  $Y$ , as should be the case if the  $x$ -fluctuations are driven by chain motions along the  $y$  direction. It would be interesting to see whether a similar relation between  $\sigma_X$  and  $V$  holds in other flows (plug flow, elongational flow, etc.) and different configurations (e.g., free polymer or attached at a single point, without wall).

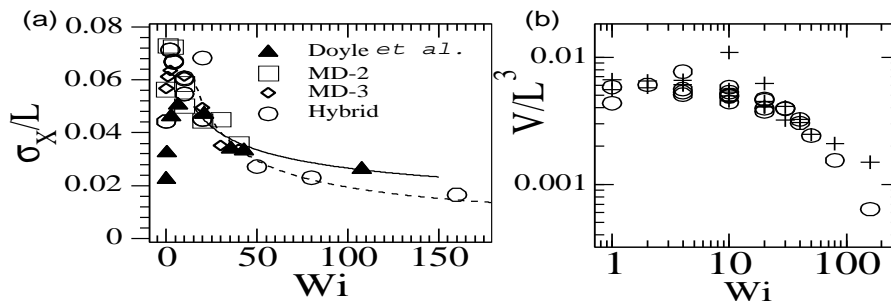


Fig. 3. (a) The standard deviation of the polymer elongation along the flow direction, normalized by the contour length  $\sigma_X/L$ . The dashed line corresponds to  $0.85 Y/L$  (calculated from our data) and the solid line to  $0.13 Wi^{-1/3}$ , which is proportional to  $Y$  for the WLC model. (b) The extensional volume of the polymer ( $V = X \times Y \times Z$ ) (circles) compared with  $0.09(\sigma_X/L)$  (crosses).

#### 4 Concluding remarks

We have analyzed the structure of a single polymer tethered to a wall undergoing shear flow in Couette geometry. Our simulations consider a freely jointed chain and explicitly include the solvent particles and the molecular nature of the wall, which attracts the polymer beads with a weak, short-ranged van der Waals attractive potential. Some simulations were carried out with a hy-

brid MD/CFD model [7], which treats the atomistic detail only around the polymer while solving the continuum momentum equation for the bulk flow. The tethered polymer is known to be quite sensitive to finite size effects and one of the purposes of this work is to demonstrate that the hybrid model can avoid them in quite small MD domains, showing perfect agreement with MD simulations in larger boxes. This means that the hybrid model can open the way to simulations where flow interacts with a complex interphase (such as in drag reduction induced by grafted polymers, crystal growth or wetting, to mention some) for which both, the atomistic details near the interphase and the macroscopic flow, play a relevant rôle.

We noticed that the polymer behaviour is altered by atomistic effects mediated by the wall. In particular, at large enough shear rates,  $\dot{\gamma}$ , the polymer width in the normal-to-wall direction ( $y$ ) becomes comparable to the bead-wall interaction length and the polymer becomes adsorbed to the wall. We also found that the extension of the flexible chain along the  $y$  direction scales with  $\dot{\gamma}$  in a manner similar to the scaling law predicted for a semiflexible chain. This fact may be due to chain compression induced by the strong layering of the solvent near the wall [7] and could be studied further by comparison with simulations without wall interactions and/or without explicit solvent. We believe that the wall-induced effects observed can be found in situations where long-range electrostatic polymer-surface interactions are important.

This research was supported by the European Commission through a Marie Curie Fellowship (HPMF-CT-2001-01210) and by the EPSRC RealityGrid project grant GR/R67699. R. D-B acknowledges support from BFM2001-0290.

## References

- [1] P. Doyle, B. Ladoux, J.-L. Viovy, Phys. Rev. Lett. 84 (2000) 4769.
- [2] B. Ladoux, P. Doyle, Eur. Phys. Lett. 52 (2000) 511.
- [3] A. S. Lemak, N. K. Balabaev, Y. N. Krnet, Y. G. Yanovsky, J. Chem. Phys. 108 (1998) 797.
- [4] P. LeDuc, C. Haber, G. Bao, D. Wirtz, Nature 399 (1999) 564.
- [5] R. Delgado-Buscalioni, P. V. Coveney, Phys. Rev. E 67 (2003) 046704.
- [6] E. G. Flekkøy, G. Wagner, J. Feder, Europhys. Lett. 52 (2000) 271.
- [7] S. Barsky, R. Delgado-Buscalioni, P. V. Coveney, J. Chem. Phys. 121 (2004) 2403.
- [8] R. Delgado-Buscalioni, P. V. Coveney, J. Chem. Phys. 119 (2003) 978.



- [9] R. Delgado-Buscalioni, P. V. Coveney, *Phil. Trans. Roy. Soc. London A* 362 (2003) 1639.
- [10] K. Kremer, G. Grest, *J. Chem. Phys.* 92 (1990) 5057.
- [11] J.W. Hatfield and R. S. Quake, *Phys. Rev. Lett.* 82 (1999) 3548.
- [12] Y. Marciano, F. Brochard-Wyart, *Macromol.* 28 (1995) 985.